Focussed on Steels and Composites for Engineering Structures

Visual Abstract

Discrete-element modeling of strain localization in a dense and highly coordinated periodic granular assembly

Trung-Kien Nguyen
Faculty of Building and Industrial Construction, Hanoi University of Civil Engineering, 55 Giai Phong road, Hanoi, Vietnam
kiennt3@nuce.edu.vn, http://orcid.org/0000-0003-0966-1617

Thanh-Trung Vo
Department of Research and International Affairs, Danang Architecture University, Danang city, Vietnam
trungvt@dau.edu.vn, https://orcid.org/0000-0003-0259-7165

Nhu-Hoang Nguyen
Faculty of Building and Industrial Construction, Hanoi University of Civil Engineering, 55 Giai Phong road, Hanoi, Vietnam
hoangnn@nuce.edu.vn

ABSTRACT. Strain localization is one of the key phenomena which has been extensively studied in geomaterials and for other kinds of materials including metals and polymers. This well-known phenomenon appears when structure/material is closed to failure. Numerous theoretical, experimental, and numerical studies have been dedicated to this subject for a long while. In the numerical aspect, strain localization inside periodic granular assembly has not been well studied in the literature. In this paper, we investigate the occurrence and development of strain localization within a dense cohesive-frictional granular assembly with high coordination number under bi-periodic boundary conditions by Discrete Element Modeling (DEM). The granular assembly is composed of 2D circular particles and subjected to biaxial loading scheme with constant lateral pressure. The results show that the formation of shear bands is of periodic type, consistent with the boundary conditions used. The occurrence and development of the shear band are originated from the irreversible loss of cohesive contacts. The latter is viewed as micro-cracking in the cohesive-frictional granular media, which is highly concentrated in the periodic shear zones and thus related to the strain localization observed at the sample scale. Finally, we also show that the strain localization is in perfect agreement with the kinematic field, displayed in terms of displacement fluctuation.

KEYWORDS. Granular materials; DEM; Strain Localization; Periodic Boundary Conditions; Displacement Fluctuation.

OPEN ACCESS

Citation: Nguyen, T-K., Vo, T-T., Nguyen, N-N., DEM investigation on strain localization in a dense periodic granular assembly with high coordination number, Frattura ed Integrità Strutturale, 59 (2022) 188-197.

Received: 20.08.2021
Accepted: 22.10.2021
Published: 01.01.2022

INTRODUCTION

Strain localization is one of the most typical problems of large deformations in geomaterials. This phenomenon appears when structure/material is close to failure. The strain localization is generally associated with the plastic deformation of the material. Localized zones are better known as shear bands; the deformation of the structure then associates with one or several shear bands. The strain localization has been generally observed at different scales: from the real scale of the structure to the scale of laboratory experiments. Regarding geomaterials, the strain localization is manifested in most laboratory tests (e.g. triaxial tests, biaxial plane strain tests). Experimental, theoretical, and numerical studies have been extensively carried out for over 30 years to get a better understanding of this phenomenon.

For soils and granular materials, the experimental studies [1–6] made it possible to draw several important conclusions which have been listed in [1]: The strain localization in form of shear bands can be observed in most laboratory tests, leading to the failure of geomaterials; The complex regimes of strain localization can arise from particular boundary conditions or loading conditions; A well-marked peak in the stress-strain curve is often considered as a sign of the occurrence of the shear band; The measurements help to identify the shear band orientation. Previous studies have also shown that strain localization is observed not only in laboratory-scale tests but also within a large-scale shear zone (the scale of the structure) [7,8].

From a theoretical standpoint, the theory of bifurcation is the reference framework for a theoretical consideration of strain localization. In this theory, the shear band is treated as a problem of loss of uniqueness of the structure mechanical solution. The emergence of a shear band must satisfy both kinematic and static conditions while respecting the constitutive law of material [9–11].

From the numerical aspect, divers' methods have been used to model the overall behavior and strain localization in granular materials [12–16]. Among them, the Discrete Element Method (DEM) has been extensively applied and proved as a powerful tool for such kinds of materials. However, wall limit boundary conditions were usually used in discrete-element modeling. In practice, since the wall effects induce disturbances in the granular structure, the condition of homogeneity and representative is not always satisfied. These undesired effects of rigid wall boundaries can be eliminated by using periodic boundary conditions (PBC). The use of the PBC allows predicting the mechanical responses of the granular sample without considering the contacts between border particles and the rigid wall. Additionally, PBC are observed to produce homogeneous, isotropic states (for isotropic stresses) and static steady state [17,18].

Although there have been many numerical studies on strain localization, the formation of the shear band inside a periodic granular assembly has not been well studied in literature so far. In this paper, we aim to tackle this aspect in finding the characteristic of macro-strain localization by using periodic boundary conditions to prevent the wall effect. Moreover, we tend to establish the linking correlation from the occurrence and development of the shear band to the micro-cracking of cohesive-frictional contact, and the displacement fluctuation field of the granular assembly. This relationship has not yet been fully reported in previous studies. In order to shed light on these interesting questions, the DEM is employed to model the behavior of dense and highly coordinated cohesive-frictional granular assembly under biaxial loading scheme and constrained by bi-periodic boundary conditions. The formation of shear bands within the granular assembly is then analyzed and discussed throughout the loading process, in both static (force chains map) and kinematic (displacement fluctuation field) aspects.

METHODOLOGY

In this paper, investigating the strain localization phenomenon in periodicity granular assembly has been performed by means of Discrete Element Modeling. We first describe the numerical procedure, micromechanical model, sample preparation process, and the principle of the biaxial compression test of the periodic granular assembly.

Discrete Element Modeling (DEM)

Discrete Element Modeling (DEM) applied to geomaterials has been developed over the last forty years since the pioneering work at the end of seventy's decade [18–22]. Various particle shapes could be treated within the DEM framework. In the present research, we limit to 2D circular particles case. In the DEM, the particles are considered as rigid bodies. The contact force law is described by normal and tangential forces, these are related to the relative displacements of grains in contact. The equation of motion is based on Newton's second law. A standard DEM approach has been employed by using the 3rd order predictor-corrector scheme.

The parameters that govern the contact interaction forces are key ingredients in DEM computation. In our case, they are normal and tangential forces. To model cohesive-frictional granular media, the normal force (f_n) is composed of the elastic part (f_{el}) and cohesive part (f_c) such as $f_n = f_{el} + f_c$ in which $f_{el} = -k_n \cdot \delta$ and $f_c = -\langle d \rangle \cdot \sigma_0$ with $\langle d \rangle$ is the mean diameter of the granular assembly and σ_0 is isotropic stress. The tangential force (f_t) is computed via the tangential stiffness (k_t) and the relative tangential displacement of particles in contact (δu_t) as $f_t^{T+\Delta T} = f_t^T + \Delta f_t^{\Delta T} = f_t^T - k_t \cdot \Delta u_t$. This tangential force is limited by the Coulomb threshold $|f_t| \le \mu \cdot f_{el}$ where μ is the intergranular coefficient of friction. The rheological model presented herein is thus an incremental elastoplastic law. The gravity force is neglected in this simulation. In this model, k_n, k_t, δ, Δu_t denote the normal, tangential stiffness, normal deflection, and relative tangential displacement, respectively.

Periodic boundary conditions (PBC)

The influence of boundary conditions is more important in modeling than in experimentation. This is primarily due to the reduced number of grains in the simulation compared to the real experiment. We can classify three types of boundary conditions, often encountered in the discrete-element modeling of granular materials: rigid or flexible wall boundaries and periodic boundary conditions. In practice, the condition of homogeneity and representative is not always satisfied, because the wall effects induce disturbances in the granular structure. These undesirable effects of the wall boundaries can be eliminated by using periodic boundary conditions. The use of the periodic cell allows mechanical responses to be predicted without taking into account the interaction of border particles with the rigid wall. Furthermore, periodic boundary conditions are observed to satisfactorily produce homogeneous and isotropic states (for isotropic stresses), and the static equilibrium [17,18,23].

As already stated, the DEM considers the individual particle's motion and the interactions between particles in the granular assembly. A standard approach, the 3rd order predictor-corrector scheme [24], is used to integrate the motion equations. The particles' characteristic is controlled by their mass, position, velocity, and acceleration. The granular assembly can be defined in 2D through the two vectors $(\vec{u}, \vec{v})$ as shown in Fig. 1. The matrix h transforms the real values into the reduced values as follows:

$$\vec{r} = h \cdot \vec{s} \tag{1}$$

$$\dot{\vec{r}} = \dot{h} \cdot \vec{s} + \dot{\vec{s}} \cdot h \tag{2}$$

Where $\vec{r}$ and $\vec{s}$ are grains' coordinates; $\dot{\vec{r}}$ and $\dot{\vec{s}}$ are grains' velocity in the real and reduced configurations, respectively. The matrix h is simply formulated by the two basis vectors that define the elementary cell in real coordinates [7,15,18]:

$$h = \begin{pmatrix} \vec{u} & \vec{v} \end{pmatrix} = \begin{pmatrix} u_1 & v_1 \\ u_2 & v_2 \end{pmatrix} \tag{3}$$

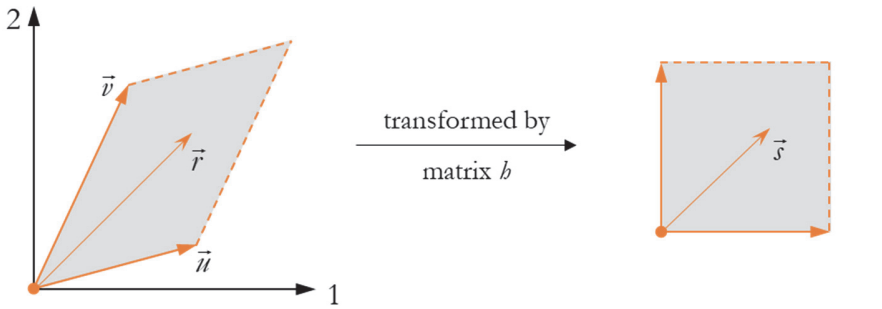

Figure 1: 2D Periodic cell defined by basis vector. The transformed vector allows to transfer from the real coordinates to the reduced coordinates and vice-versa. The reduced coordinates is an orthonormal system with value limits from 0 to 1.

With PBC, the particles at the border of the elementary cell (grey cell in Fig. 2 (left)) may interact with the image particles in the neighboring cell (white cell in Fig.2 (left)). It is, for example, the case of particles n and m in Fig. 2 (right) with n' is the image of particle n. In this way, the PBC allow to extend the system to infinity.

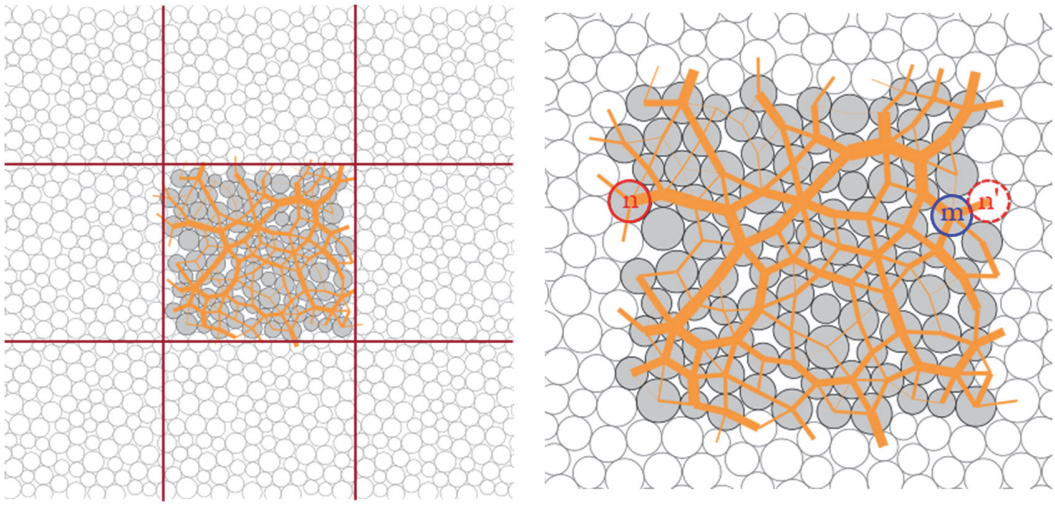

Figure 2: Periodic boundary conditions (PBC): elementary cell in grey and its neighbors (left); close view with a highlight on the interaction between real and image particle (right).

Sample preparation process

The sample preparation process plays an important role because it affects the mechanical properties and the behavior of granular assembly. In the present paper, we focus only on the case of dense and highly coordinated cohesive-frictional granular materials. A dense granular assembly can be thus obtained by setting zero coefficient of friction during the isotropic compression stage. A detailed analysis of the non-zero coefficient of friction on the density of granular assembly behavior has been reported in [7].

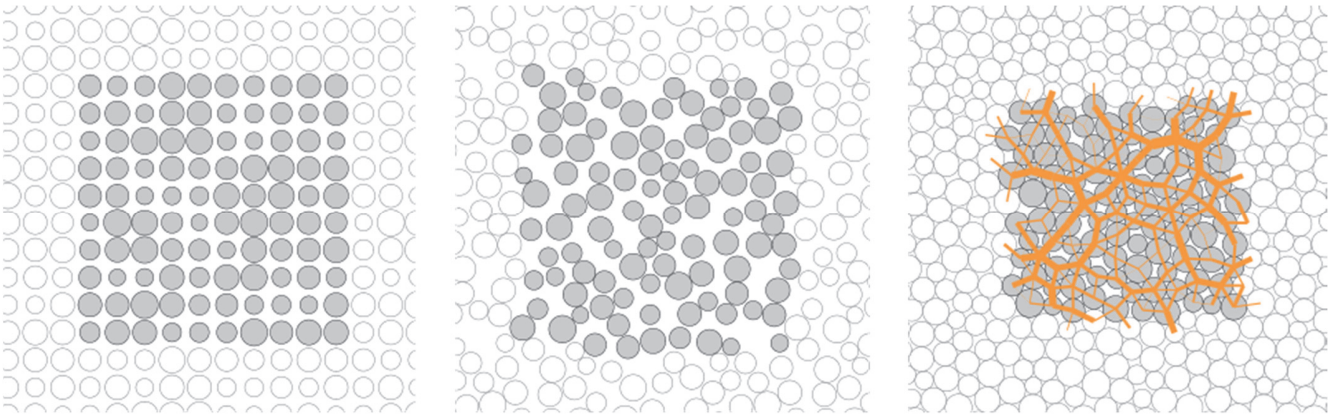

Figure 3: Sample generation and isotropic compression stage: (a) grid of particles; (b) granular assembly after shaking by random velocity field and (c) granular assembly after isotropic compression

Before the isotropic compression stage, the granular assembly had been generated as follows: a set of particles with a given number of particles (npa) and size distribution $[r_{min}, r_{max}]$ are placed in a rectangular grid. Their radius was determined by using a random generator while respecting a uniform distribution (Fig. 3(a)). The granular set was assigned a random velocity field. The particles moved and interacted as rigid bodies without any energy dissipation in this step Fig. 3(b). Finally, the granular packing was subjected to the isotropic compression of which the forces chain map at the final equilibrium state is illustrated in Fig. 3(c).

Biaxial loading scheme

After being generated, the granular sample is subjected to isotropic loading up to the desired isotropic stress σ_0. To perform biaxial loading, we then apply a constant axial strain rate with a constant lateral pressure which is equal to the isotropic stress σ_0. The constant axial strain rate is applied via the inertial number (I) as described in [7,25]. In this simulation, an inertial number $I = 10^{-4}$ (equivalent to approximately 0.006% in axial strain increment) is used to ensure the quasi-static loading. The principle of the biaxial loading scheme and illustration of the periodic boundary conditions applied to the granular assembly is schematized in Fig. 4.

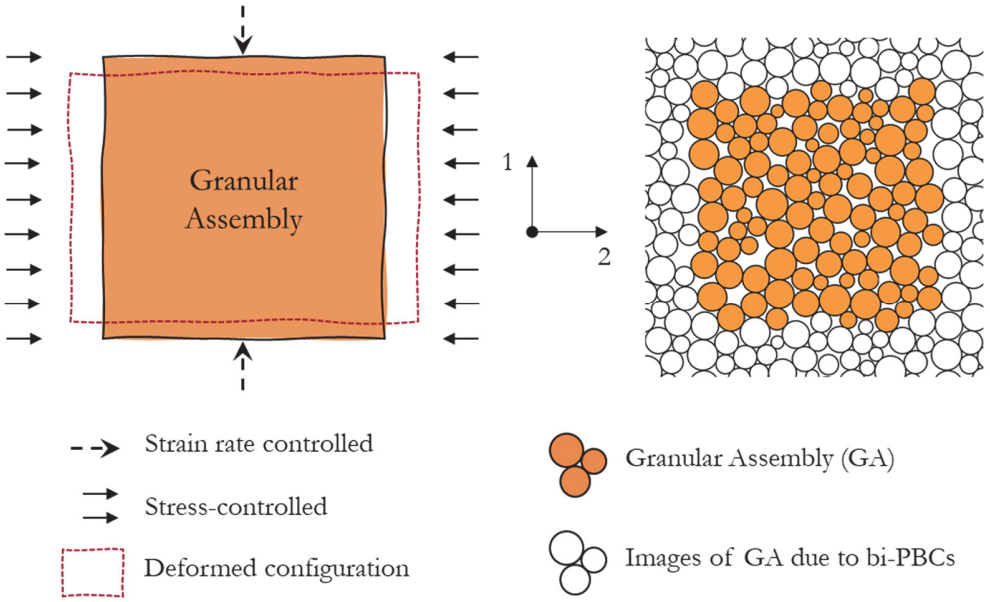

Figure 4: Principle of biaxial loading (left) and granular assembly with bi-PBC (right).

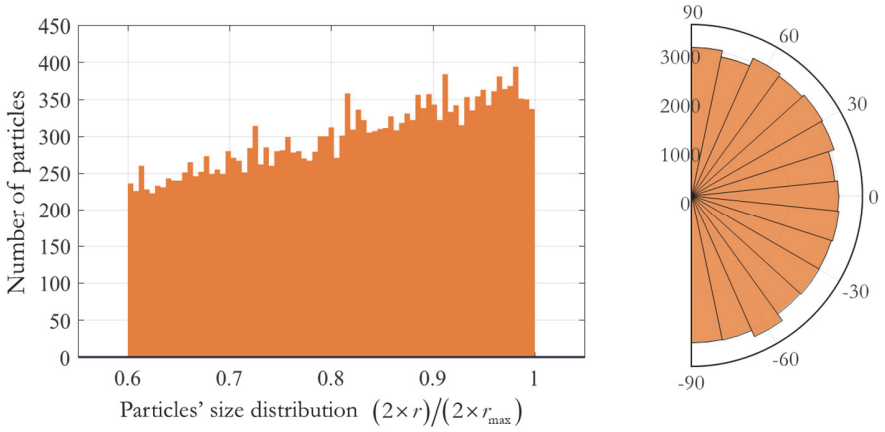

Figure 5: Particle diameter distribution (left) and contact orientation at isotropic state (right).

STRAIN LOCALIZATION IN DENSE PERIODIC GRANULAR ASSEMBLY

In this work, a granular assembly, which composes of 22.500 circular particles, is used. We first prepared a sample based on the procedure discussed above. The particle size of the granular assembly is varied in a range $r_{max}/r_{min} = 5/3$. The sample was then subjected to isotropic loading with zero coefficient of friction ($\mu = 0.0$) to obtain a dense granular

packing. At the isotropic state, the granular sample's void ratio index is $e = 0.20$. The coordination number z, which is defined as the average number of contacts ($ncont$) per grain, implying $z = 2 \times ncont / npa = 4.2$. Particles' size distribution and contact orientation at the isotropic state are presented in Fig. 5. It can be seen that the particle radii distribution is followed a uniform law distribution. Contact orientation is almost isotropic. To investigate the strain localization phenomenon of periodic granular assembly, we perform biaxial loading with constant lateral pressure and constant axial strain rate as described in the previous section. The micromechanical parameters used in the biaxial simulation involve the stiffness number $\kappa = k_n / (\sigma_0 \cdot \langle d \rangle) = 1000$, the ratio between normal and tangential stiffness $k_n / k_t = 1$, and the intergranular coefficient of friction $\mu = 0.5$. The cohesive contact force is compared to the initial isotropic stress such as $f_c = -\langle d \rangle \cdot \sigma_0$. It is important to note that all the contact are initially cohesive. As the loading progresses, the deformation leads to the degradation of cohesion when contact separation occurs. The degradation of cohesion is of irreversible type. This means that when the contact cohesion is degraded, the cohesion could not be retrieved even when new contacts are formed.

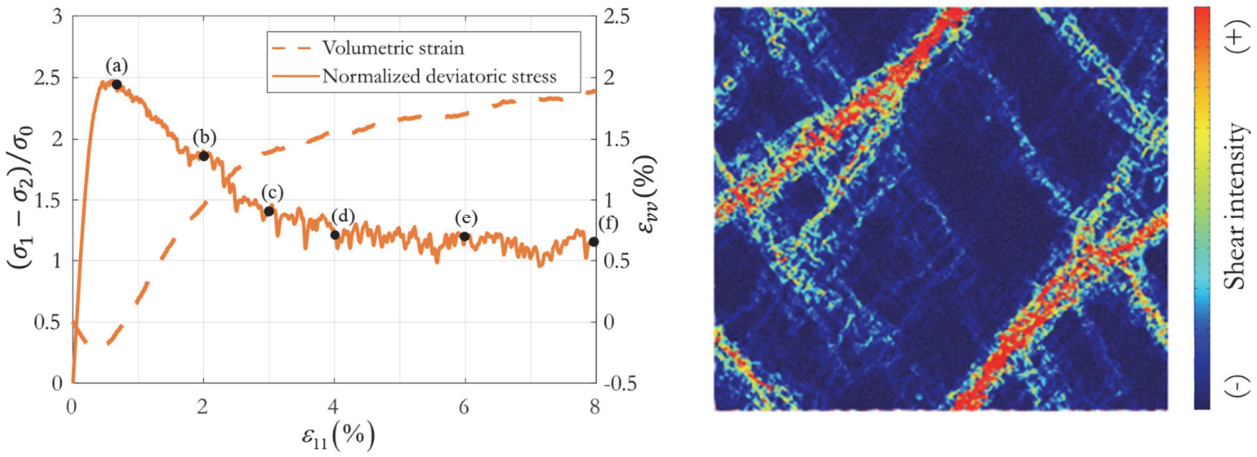

Figure 6: Stress-strain behavior (left) and the second invariant strain tensor for the final instant $\varepsilon_{11} = 8.0\%$ of biaxial loading (right).

Fig. 6 (left) shows the evolution of normalized deviatoric stress $(\sigma_1 - \sigma_2)/\sigma_0$ and volumetric strain (ε_{vv}) as a function of axial strain ε_{11}, and the second invariant of strain tensor field. One can notice that the obtained behavior of granular assembly is typical of granular soil represented by pre-peak, peak, and post-peak regimes. Since the sample is initially very dense and highly coordinated, the peak in stress-strain behavior is rapidly found at $\varepsilon_{11} = 0.8\%$. After passing the peak, the granular assembly behavior represents a softening phase before reaching the residual state from 4.0% of axial strain. At the final stage, the void ratio of the granular sample is $e = 0.23$ and the coordination number reduces to $z = 3.5$. To verify the occurrence of the shear band within the granular sample, the picture on the right-hand side of Fig. 6 shows the second invariant of strain tensor for the final instant $\varepsilon_{11} = 8.0\%$. This figure indicates the formation of the shear band in periodic form with two principal shear bands located at approximately 40° to the horizontal axis.

It is well-known that intergranular cracking leads to the failure of the specimen. In the following discussion, we show that inside the shear zone, most of the cohesive links are broken, i.e. intergranular crackings occur. Fig. 7 presents the map of the force chains corresponding to several loading instants (points a to f) as indicated in Fig. 6 (left). As a reminder, the micromechanical model used in this simulation is able to account for the degradation of cohesion at the contact level. All the contacts are initially cohesive, but the loading induces the degradation of cohesion, in particular in large deformation. Once the cohesion is broken, it is not reversible even when new contacts are formed (irreversible cohesion). The degradation of cohesive contacts is considered as the intergranular cracking (micro-cracking) that occurs inside the cohesive-frictional granular media.

In the force chains map, the elastic normal force f_{el} is represented in such a manner that the width of the lines joining the centers of the interacting particles is proportional to the intensity of the elastic force. To highlight the zone with/without cohesion, color notation is distinguished in Fig. 7, contact with cohesion in grey, and contact without cohesion in orange. As the loading increases, the intergranular cracking initiates and propagates throughout the granular assembly. The

coalescence of micro-crackings leads to the initiation and development of the shear band. At the final stage of the biaxial loading ($\varepsilon_{11} = 8.0\%$), it can be seen that the contacts which lose cohesion are concentrated in the narrow bands shown in orange color. Shear band positions are periodic due to PBC applied to the sample, which is nicely consistent with the localized signatures observed in Fig. 6 (right). At the stress-strain peak (point a), the formation of the shear band is not very visible although there is a large number of contacts that already lose cohesion. Visualization becomes more and more prominent from point c (equivalent to axial strain $\varepsilon_{11} = 3.0\%$). At point e ($\varepsilon_{11} = 6.0\%$) and point f ($\varepsilon_{11} = 8.0\%$), a high concentration of intergranular cracking is recognized in the shear band zones (narrow orange zones). The heterogeneity of the granular sample is obvious. A zoom-in shear zone is displayed in Fig. 8. It can be seen that the larger of the shear zone is composed of several grains. Although a high intensity of micro-cracking is observed inside the shear band, it should be noted that there are still many intact contacts, i.e. the contact of which the cohesion has remained (grey lines in between two dashed inclined lines in Fig.8 (right)).

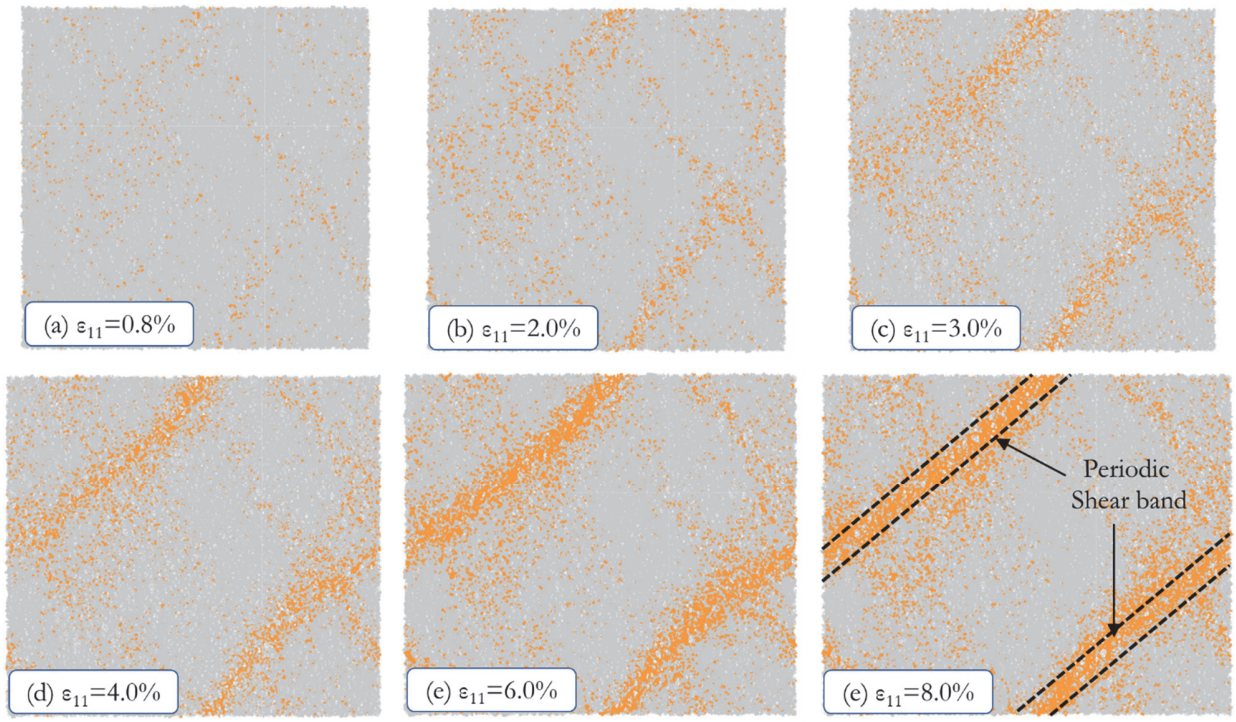

Figure 7: Force chain maps. The thickness of the force chain is proportional to the elastic normal contact force f_{el}. Color convention: grey (with cohesion) and orange (no cohesion).

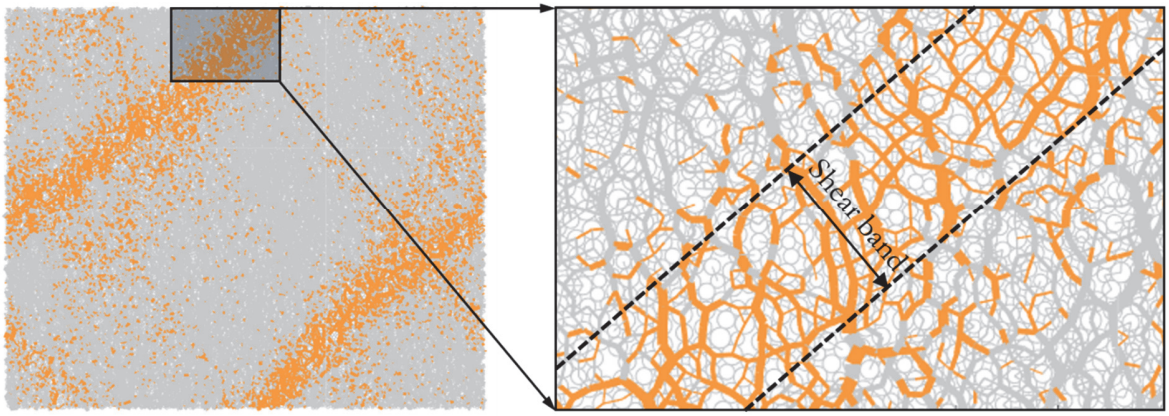

Figure 8: Zoom-in shear band showing the concentration of intergranular crackings inside the shear zone. Color convention: grey (with cohesion) and orange (no cohesion).

The displacement fluctuation vector ($\delta\vec{u}$) [26] is defined as the difference between the displacements of the particles ($\vec{u}$) and the product between the strain field predicted by the Mechanics of Continuum Media ($\underline{\underline{\varepsilon}}$) and the position of the particles ($\vec{r}$). Its expression can be written as:

$$\delta\vec{u} = \vec{u} - \underline{\underline{\varepsilon}} \cdot \vec{r} \tag{4}$$

In this way, by excluding the impact of macroscopic strain, the displacement fluctuation is the non-affine component of the displacement field [26,27]. The strain field is simply determined thanks to the dimensions of granular assembly while particles' position is recorded for every time step, enabling the possibility of determining grain displacement.
The displacement fluctuation field shown in Fig. 9 is in nice agreement with the chains of forces presented in Fig. 7. The periodic bands occur and develop in the same positions. However, it seems that the interpretation of shear bands by the fluctuations is more prominent. Inside the periodic shear bands, the particles' displacement fluctuation vectors are opposed. This image looks like two blocks are sliding over each other. As point out by [28], displacement fluctuations in granular materials are a direct manifestation of grain rearrangement. This is the origin of irreversible strain, together with irreversible cohesion used in this model. This important feature plays an important role that linking the strain localization at the macro-scale to the microscopic properties. The latter is statically and kinematically demonstrated in this paper in terms of intergranular cracking and displacement fluctuation field.

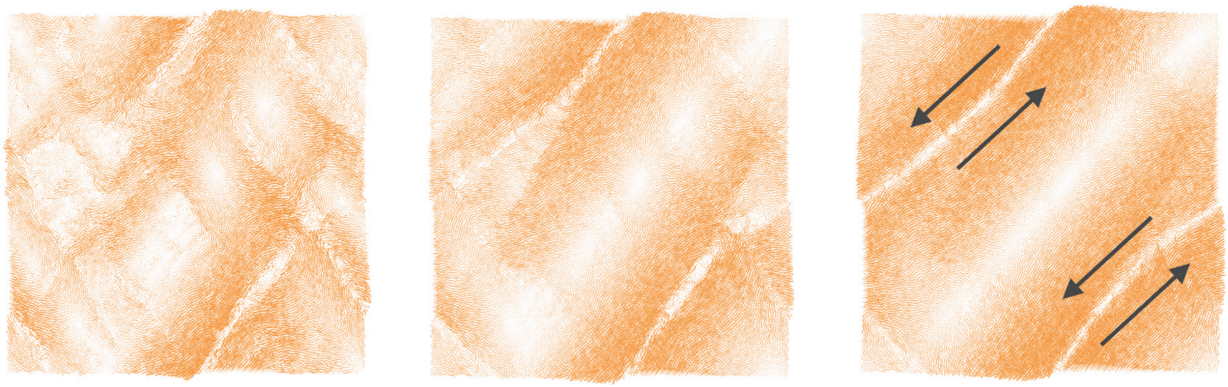

(a) ε_{11}=0.8% (b) ε_{11}=3.0% (c) ε_{11}=8.0%

Figure 9: Strain localization in terms of displacement fluctuation field.

CONCLUSIONS

A numerical investigation on the strain localization in a dense cohesive-frictional granular media with high coordination number under bi-periodic boundary conditions has been carried out in this paper. First, the Discrete Element Modeling (DEM) methodology, sample preparation process, and interaction contact laws were addressed. Then, we presented the biaxial loading scheme with the bi-periodic boundary conditions (BPC).
Biaxial numerical simulations by DEM with bi-PBC have been successfully performed on a granular sample composed of 22.500 circular particles. The sample was initially very dense (void ratio index $e = 0.20$) and highly coordinated (coordination number $z = 4.2$). We have studied how the strain localization phenomenon manifests in cohesive-frictional granular media modeled by DEM. The numerical results clearly showed that the occurrence of the shear band is of periodic type, consistent with the boundary conditions used in the simulation.
To get further insight into both static and kinematic aspects that induce macro strain localization, we have considered the force chains representing the degradation of the cohesion at contact level (static aspect), and the displacement fluctuation field (kinematic aspect). By comparing both static and kinematic observations to the shear bands shown by the second invariant strain map, the results confirmed that the particles' kinematic and cohesive contact degradation mechanism characterize the failure mode, the shear band occurrence and development. Remarkably, the shear band formation is donated by the concentration of micro-intergranular cracking (cohesive contact broken) in periodic narrow zones, which is in nice agreement with the displacement fluctuation field.

ACKNOWLEDGMENT

The authors acknowledge the support from Hanoi University of Civil Engineering, Vietnam through research project no. 34-2021/KHXD-TĐ.

REFERENCES

[1] Han, C., Vardoulakis, I. (1991). Plane-strain compression experiments on water-satured fine-grained sand, Geotechnique, 41(1), pp. 49–78, DOI: 10.1680/geot.1991.41.1.49.
[2] Vardoulakis, I., Goldscheider, M., Gudehus, G. (1978). Formation of shear bands in sand bodies as a bifurcation problem, Int. J. Numer. Anal. Methods Geomech., pp. 99–128, DOI: 10.1002/nag.1610020203.
[3] Finno, R.J., Harris, W.W., Mooney, M.A., Viggiani, G. (1997). Shear bands in plane strain compression of loose sand, Geotechnique, 47(1), pp. 149–65, DOI: 10.1680/geot.1997.47.1.149.
[4] Desrues, J., Viggiani, G. (2004). Strain localization in sand: an overview of the experimental results obtained in grenoble using stereophotogrammetry, Int. J. Numer. Anal. Methods Geomech., 28, pp. 278–321, DOI: 10.1002/nag.338.
[5] Desrues, J., Lanier, J., Stutz, P. (1985). Localization of the deformation in tests on sand sample, Eng. Fract. Mech., 21, pp. 909–21, DOI: 10.1016/0013-7944(85)90097-9.
[6] Bésuelle, P., Desrues, J., Raynaud, S. (2000). Experimental characterisation of the localisation phenomenon inside a Vosges sandstone in a triaxial cell, Int. J. Rock Mech. Min. Sci., 37, pp. 1223–1237, DOI: 10.1016/S1365-1609(00)00057-5.
[7] Nguyen, T.K. (2013). Modélisation multi-échelle des matériaux granulaires frottant-cohésifs. Université de Grenoble-Alpes.
[8] Ebert, A., Herwegh, M., Pfiffner, A. (2007). Cooling induced strain localization in carbonate mylonites within a large-scale shear zone (Glarus thrust, Switzerland), J. Struct. Geol., 29(7), pp. 1164–1184, DOI: 10.1016/j.jsg.2007.03.007.
[9] Rice, J. (1976).The localization of plastic deformation. 14th International Congress on Theoretical and Applied Mechanics, vol. 1, North-Holland Publishing Company, pp. 207–220.
[10] Rudnicki, J.W., Rice, J.R. (1975). Conditions for the localisation of the deformation in pressure sensitive dilatant materials, J. Mech. Phys. Solids, 23, pp. 371–394, DOI: 10.1016/0022-5096(75)90001-0.
[11] Desrues, J., Chambon, R. (2002). Shear band analysis and shear moduli calibration, Int. J. Solids Struct., 39(13–14), pp. 3757–3576, DOI: 10.1016/S0020-7683(02)00177-4.
[12] Argilaga, A., Desrues, J., Dal Pont, S., Combe, G., Caillerie, D. (2018). FEM×DEM multiscale modeling: Model performance enhancement from Newton strategy to element loop parallelization, Int. J. Numer. Methods Eng., 114(1), DOI: 10.1002/nme.5732.
[13] Nguyen, T.K., Claramunt, A.A., Caillerie, D., Combe, G., Dal Pont, S., Desrues, J., Richefeu, V. (2017).FEM × DEM: A new efficient multi-scale approach for geotechnical problems with strain localization. EPJ Web of Conferences, vol. 140.
[14] Nguyen, T.K., Combe, G., Caillerie, D., Desrues, J. (2014). FEM × DEM modelling of cohesive granular materials: Numerical homogenisation and multi-scale simulations, Acta Geophys. 62(5), DOI: 10.2478/s11600-014-0228-3.
[15] Nguyen, T.K. (2020). Multi-scale modeling of geomechanics problems using coupled finite-discrete element method, J. Sci. Technol. Civ. Eng. (STCE)-NUCE, 14(1V), pp. 93–103.
[16] Desrues, J., Argilaga, A., Caillerie, D., Combe, G., Nguyen, T.K., Richefeu, V., Dal Pont, S. (2019). From discrete to continuum modelling of boundary value problems in geomechanics: An integrated FEM-DEM approach, Int. J. Numer. Anal. Methods Geomech., 43(5), DOI: 10.1002/nag.2914.
[17] Radjai, F. (2018). Multi-periodic boundary conditions and the Contact Dynamics method, Comptes Rendus Mécanique, 346(3), pp. 263–277, DOI: 10.1016/j.crme.2017.12.007.
[18] Radjai, F., Dubois, F. (2011). Discrete-element modeling of granular materials, Wiley.
[19] Cundall, P.A., Strack, O.D. (1979). A disrete numerical model for granular assemblies, Geotechnique, 29, pp. 47–65, DOI: 10.1680/geot.1979.29.1.47.
[20] Dubois, F., Acary, V., Jean, M. (2018). The Contact Dynamics method: A nonsmooth story, Comptes Rendus Mécanique, 346(3), pp. 247–262, DOI: 10.1016/j.crme.2017.12.009.
[21] Nguyen, T.K., Desrues, J., Combe, G., Nguyen, D.H. (2020). A numerical homogenized law using discrete element

method for continuum modelling of boundary value problems, Lect. Notes Civ. Eng., 54, DOI: 10.1007/978-981-15-0802-8_113.

[22] Vo, T.-T., Nguyen, C.T., Nguyen, T.-K., Nguyen, V.M., Vu, T. Lo. (2021). Impact dynamics and power-law scaling behavior of wet agglomerates, Comput. Part. Mech., , pp. 1–14, DOI: 10.1007/s40571-021-00427-9.

[23] Borja, R.I., Wren, J.R. (1995). Micromechanics of granular media Part I: Generation of overall constitutive equation for assemblies of circular disks, Comput. Methods Appl. Mech. Eng., 127(1–4), pp. 13–36, DOI: 10.1016/0045-7825(95)00846-2.

[24] Allen, M.P., Tildesley, D.J. (1987). Computer Simulation of Liquids, Oxford University Press.

[25] Nguyen, T.-K. (2021). On the Representative Volume Element of Dense Granular Assemblies Made of 2D Circular Particles, Struct. Heal. Monit. Eng. Struct., , pp. 499–508, DOI: 10.1007/978-981-16-0945-9_41.

[26] Roux, J.-N., Combe, G. (2003). On the meaning and microscopic origins of quasistatic deformation of granular materials, Proc. 16th ASCE Eng. Mech. Conf., Paper No.(May 2014), pp. 1–5.

[27] Roux, J.-N., Combe, G. (2002). Quasistatic rheology and the origins of strain, Comptes Rendus Phys., 3, pp. 131–140.

[28] Richefeu, V., Combe, G., Viggiani, G. (2012). An experimental assessment of displacement fluctuations in a 2D granular material subjected to shear, Geotech. Lett., 2(3), pp. 113–118, DOI: 10.1680/geolett.12.00029.